

# Synaptic Activity and Nuclear Calcium Signaling Protect Hippocampal Neurons from Death Signal-associated Nuclear Translocation of FoxO3a Induced by Extrasynaptic *N*-Methyl-D-aspartate Receptors\*

Received for publication, March 26, 2010, and in revised form, April 16, 2010. Published, JBC Papers in Press, April 19, 2010, DOI 10.1074/jbc.M110.127654

Oliver Dick and Hilmar Bading<sup>1</sup>

From the Department of Neurobiology, Interdisciplinary Center for Neurosciences (IZN), University of Heidelberg, 69120 Heidelberg, Germany

Synaptic activity and the generation of nuclear calcium signals promote neuronal survival through a transcription-dependent process that is not fully understood. Here we show that one mechanism of activity-induced acquired neuroprotection involves the Forkhead transcription factor, FoxO3a, which is known to induce genomic death responses upon translocation from the cytosol to the nucleus. Depletion of endogenous FoxO3a using RNA interference renders hippocampal neurons more resistant to excitotoxic cell death. Using a FoxO3a-green fluorescent protein (GFP) fusion protein to monitor in real time the localization of FoxO3a in hippocampal neurons, we found that several cell death inducing stimuli, including the stimulation of extrasynaptic *N*-methyl-D-aspartate receptors, growth factor withdrawal, and oxygen-glucose deprivation, caused a swift translocation of FoxO3a-GFP from the cytosol to the cell nucleus. This translocation was inhibited in hippocampal neurons that had undergone prolonged periods of synaptic activity before exposure to cell death-inducing conditions. The activity-dependent protection from death signal-induced FoxO3a-GFP nuclear translocation required synaptic *N*-methyl-D-aspartate receptor activation and was dependent on nuclear calcium signaling and calcium/calmodulin-dependent protein kinase IV. The modulation of nucleo-cytoplasmic shuttling of FoxO3a may represent one mechanism through which nuclear calcium-induced genomic responses affect cell death processes.

Nuclear calcium has emerged as a key signal in activity-induced adaptive responses, including learning and memory and acquired neuroprotection (1–8). The latter term defines a process that renders neurons that have undergone periods of neuronal activity more resistant to harmful, cell death-inducing conditions (1, 3, 4). Acquired neuroprotection is triggered by calcium entry into neurons through synaptic NMDA<sup>2</sup> recep-

tors and requires calcium transients to invade the cell nucleus and the activation or repression of gene transcription (1, 3, 4, 6, 7). Several activity- and nuclear calcium-regulated genes with neuroprotective potential have been identified (6, 7). However, the processes through which nuclear calcium-regulated genomic events boost neuronal survival activity are not understood. In this study we considered the possible role of FoxO3a in acquired neuroprotection. FoxO3a is a member of the class O subgroup of the Forkhead transcription factor family, which is expressed in many different tissues and involved in mediating the effects of insulin and growth factors on several cellular processes including cell cycle progression, glucose metabolism, and apoptosis (9–18). The activity of FoxO3a as a transcriptional regulator is primarily, although not exclusively, controlled by its subcellular localization (19). In the absence of growth- or neurotrophic factors, FoxO3a may localize to the cell nucleus, causing transcriptional induction of cell death-promoting genes including Fas ligand (Fas-L) (20), the Bcl-2 interacting mediator of cell death (Bim) (21, 22), the tumor necrosis factor-related apoptosis-inducing ligand (TRAIL) (23), and other FoxO genes (24). Activation of the phosphoinositide 3-kinase-Akt pathway and phosphorylation of FoxO3a by Akt (also known as protein kinase B) causes FoxO3a to be released from the DNA and exported from the nucleus in a Crm-1- and 14-3-3-dependent manner (10, 11, 25). The removal of Akt-phosphorylated FoxO3a from the nucleus and the disruption of FoxO3a-mediated transcription of pro-death genes are thought to underlie the neuroprotective activity of phosphoinositide 3-kinase-Akt signaling (20) and, more generally, may represent an evolutionary conserved mechanism controlling cell resistance to stress and life span (26, 27). Here we describe the observation that in hippocampal neurons the nucleo-cytoplasmic shuttling of FoxO3a is antagonistically controlled by stimuli that activate synaptic *versus* extrasynaptic NMDA receptors. Moreover, synaptic activity-induced nuclear calcium transients cause

\* This work was supported by the Alexander von Humboldt Foundation (Wolfgang-Paul Prize (to H.B.)), European Union Project GRIPANNT, the European Union Network of Excellence NeuroNE, the Sonderforschungsbereich (SFB) 488, and an European Research Council Advanced Grant (to H. B.).

<sup>1</sup> A member of the Excellence Cluster *CellNetworks* at Heidelberg University. To whom correspondence should be addressed: Dept. of Neurobiology, Interdisciplinary Center for Neurosciences, University of Heidelberg, Im Neuenheimer Feld 364, 69120 Heidelberg, Germany. Tel.: 496221-54-8218; E-mail: hilmar.bading@uni-hd.de.

<sup>2</sup> The abbreviations used are: NMDA, *N*-methyl-D-aspartate; GFP, green fluo-

rescent protein; shRNA, short hairpin RNA; CaMKII, calcium/calmodulin-dependent protein kinase II; JNK, c-Jun N-terminal kinase; DUSP, dual-specificity phosphatases; OGD, oxygen-glucose deprivation; ANOVA, analysis of variance; MAP, mitogen-activated protein; AP, action potential; MCPG, alpha-methyl-4-carboxyphenylglycine; rAAV, recombinant adeno associated virus; APV, 2-amino-5-phosphonopentanoic acid; GABA,  $\gamma$ -aminobutyric acid.

hippocampal neurons to build up a protective shield that can inhibit death signal-induced nuclear translocation of FoxO3a.

## EXPERIMENTAL PROCEDURES

**Hippocampal Cultures**—Hippocampal neurons from new born Sprague-Dawley rats were cultured as described (28), except that growth medium was supplemented with B27 (Invitrogen), 1% rat serum, and 1 mM glutamine. Neurons were plated onto 12-mm glass coverslips or plastic 4-well dishes at a density between 400 and 600 cells per mm<sup>2</sup>. Experiments were performed after a culturing period of 11–13 days during which hippocampal neurons develop a rich network of processes, express functional NMDA-type and  $\alpha$ -amino-3-hydroxy-5-methyl-4-isoxazole propionic acid/kainate-type glutamate receptors, and form synaptic contacts (1, 29, 30). The following chemicals were used: SB203580 (Calbiochem), bicuculline (Axxora, Lörrach, Germany), cyclosporine A, actinomycin D, glutamate, and NMDA (Sigma), MK-801 and MCPG (Tocris, Ellisville, MO), APV (Biotrend, Zurich, Switzerland), okadaic acid (Enzo Life Sciences, Lörrach, Germany), c-Jun N-terminal kinase (JNK) inhibitor I (BIOSOURCE, Nivelles, Belgium), Hoechst 33258 (Serva, Heidelberg, Germany).

**Recombinant Adeno-associated Viruses**—Recombinant viruses for the expression of short hairpin RNAs (shRNAs), containing the U6 promoter for shRNA expression and a calcium/calmodulin-dependent protein kinase II (CaMKII) promoter driving mCherry expression, were generated as described previously (31). To construct rAAVs for expression of shRNAs, oligonucleotides that contain the following sequences were synthesized, annealed, and cloned into the BamHI and HindIII sites of the rAAV vector: 5'-CAACCTGTCAGTGCATAGT-3' (rAAV-FoxO3a-RNAi, sense), 5'-ACTATGCAGTGACAGGTTG-3' (rAAV-FoxO3a-RNAi, antisense) (32), 5'-CGTCGCTTACCGATTTCAGAAT-3' (rAAV-control-RNAi, sense), and 5'-ATTCTGAATCGGTAAGCGACG-3' (rAAV-control-RNAi, antisense) (6, 7, 31). All rAAV vectors were generated by standard molecular biology techniques and verified by sequencing. Viral particles were produced and purified as described previously (6, 7, 31).

**Antibodies and Immunological Analyses**—Immunoblots were done using standard procedures and the following antibodies: rabbit antibody against FoxO3a (GeneTex, Irvine, CA) and a mouse antibody against tubulin (Sigma). For immunocytochemical detection of the endogenous FoxO3a, a monoclonal antibody to FoxO3a (Sigma) and a fluorescent dye-labeled secondary anti-mouse antibody were used. The localization of FLAG-tagged CaMBP4 and FLAG-tagged CaMKIV(K75E) was determined using a monoclonal antibody against the FLAG tag (Sigma) and a fluorescent dye-labeled secondary anti-mouse antibody.

**Transfection of Hippocampal Neurons**—Neurons were transfected at days *in vitro* 9 using Lipofectamine 2000 (Invitrogen), which typically yielded transfection efficiencies of 0.1–0.5% of the cell population. The FoxO3a-GFP construct used in this study was generated by cutting the pGL4.74 (hRluc/TK) vector (Promega) with HindIII and XbaI and replacing the hRluc sequence with the FoxO3a-GFP sequence (a plasmid contain-

ing the FoxO3a-GFP coding sequence was a kind gift from Dr. M. P. Smith). The sequence was confirmed by DNA sequencing. The constructs encoding the negative interfering mutant of the calcium/calmodulin (CAM)-dependent protein kinase IV (CaMKIV(K75E)) and the CaM-binding peptide (CaMBP4) have been described (6, 7, 33, 34). The expression vector for a red fluorescence protein was a kind gift from Dr. Thomas Dresbach.

**Analysis of FoxO3a-GFP Nucleo-cytoplasmic Shuttling**—To induce FoxO3a-GFP translocation, hippocampal neurons were treated with glutamate or NMDA or were subjected to trophic deprivation by transferring them from growth medium to medium containing 10% minimum Eagle's medium (Invitrogen) and 90% salt-glucose-glycine (SGG) solution (114 mM NaCl, 5.3 mM KCl, 1 mM MgCl<sub>2</sub>, 2 mM CaCl<sub>2</sub>, 10 mM HEPES (pH 7.4), 1 mM glycine, 30 mM glucose, 0.5 mM sodium pyruvate, 26.1 mM NaHCO<sub>3</sub>, and 0.001% mM phenol red; mM 325 mosmol/liter osmolarity (35)). For the induction of oxygen-glucose deprivation (OGD), cells were washed three times with deoxygenated glucose-free salt solution (containing 140.1 mM NaCl, 5.3 mM KCl, 1.0 mM MgCl<sub>2</sub>, 2.0 mM CaCl<sub>2</sub>, 10.0 mM HEPES (pH 7.4), 10 mM glycine, and 0.5 mM sodium pyruvate) and then transferred to an anaerobic chamber containing a 5% CO<sub>2</sub>, 95% N<sub>2</sub> atmosphere. Control cultures were kept for the same time in oxygenated transfection medium (35). Transfection medium consists of 10% minimum Eagle's medium (Invitrogen), 90% salt-glucose-glycine, and a supplement of 7.5  $\mu$ g of insulin/ml, 7.5  $\mu$ g of transferrin/ml, and 7.5 ng of sodium selenite/ml (Sigma). After induction of FoxO3a-GFP translocation, the neurons were fixed with phosphate-buffered saline containing 4% paraformaldehyde, 4% sucrose followed by analysis of the FoxO3a-GFP fluorescence.

**Live Imaging**—Hippocampal neurons were imaged using a Leica SP2 confocal microscope with an HCX PL APO CS 40.0  $\times$  1.25 NA oil UV objective (Leica, Wetzlar, Germany). Neurons seeded on coverslips were mounted in a perfusion chamber (LIS, Reinach, Switzerland) and were imaged at 37 °C. The visual field was chosen such that two-four FoxO3a-GFP-expressing cells were visible. Stacks spanning the whole cell body were scanned every minute to document changes in FoxO3a-GFP localization. For the evaluation one focal plane of the z-stacks showing cytoplasm and nucleus over the total time of the experiment was chosen. Fluorescence intensity for cytoplasmic and nuclear areas were measured using the open source software ImageJ, and the ratio of nuclear *versus* cytoplasmic was calculated for every time point and plotted.

Localization of FoxO3a-GFP in fixed and Hoechst 33258 stained hippocampal neurons was evaluated with a Leica DMIRBE microscope (Leica) at 40 $\times$  magnification. Localization of FoxO3a-GFP was classified as cytoplasmic if the nucleus was detectable as a dark spot surrounded by brightly fluorescent cytoplasm or as nuclear if the GFP signal in the nucleus was as bright or brighter as the cytoplasm. For each experimental condition in each experiment 300–500 transfected cells were evaluated. The percentage of FoxO3a-GFP-positive cells showing a nuclear localization was calculated. The results are given as the means  $\pm$  S.E. from at least three independent experiments. Statistical significance was determined by ANOVA.

## Nuclear Calcium and FoxO3a Shuttling

**NMDA-induced Neuronal Cell Death**—The induction and analysis of NMDA-induced neuronal cell death was done as described (1, 36). Briefly, the cells were treated with 10  $\mu\text{M}$  NMDA for 1 h at 37  $^{\circ}\text{C}$ , washed 3 times with transfection medium, and incubated at 37  $^{\circ}\text{C}$  for 12 h. After fixation, the percentage of dead cells was determined by analyzing Hoechst 33258-stained nuclei.

**Bicuculline/MK-801 Protocol to Isolate Extrasynaptic NMDA Receptors**—The protocol to isolate extrasynaptic NMDA receptors has been described (1, 36). Briefly, synaptic NMDA receptors were activated via bath application of 50  $\mu\text{M}$  bicuculline (to induce action potential bursting) for 5 min and then blocked for 10 min with 10  $\mu\text{M}$  MK-801. Unbound MK-801 was washed out by 5 medium changes with transfection medium followed by the application of 10  $\mu\text{M}$  NMDA for 1 h. Analysis of the localization of FoxO3a-GFP was done as described above.

## RESULTS

**Depletion of FoxO3a Protects against NMDA-induced Cell Death**—We first investigated the role of FoxO3a in excitotoxic cell death of hippocampal neurons. RNA interference (RNAi) was used to inhibit expression of FoxO3a. A DNA sequence encoding a shRNA designed to an appropriate target region of the mouse FoxO3a mRNA (32) was inserted downstream of the U6 promoter of an rAAV vector that also harbors an expression cassette for *mCherry*. To control for nonspecific effects of infections with rAAVs carrying an expression cassette for shRNAs, an rAAV was used that contains a control shRNA, which has no significant sequence similarity to the mouse, rat, or human genome. For both rAAV-FoxO3a-RNAi and rAAV-control-RNAi, infection rates of 80–95% of neuron population were obtained (data not shown). Immunoblot analysis revealed that infection of hippocampal neurons with rAAV-FoxO3a-RNAi but not with rAAV-control-RNAi was effective in reducing expression of FoxO3a (Fig. 1A). Neither infection with rAAV-FoxO3a-RNAi nor with rAAV-control-RNAi led to a reduction of FoxO1, FoxO4, or FoxO6 protein expression in hippocampal neurons (data not shown). The lack of effect of rAAV-FoxO3a-RNAi on FoxO1, FoxO4, or FoxO6 protein expression indicates specificity of the FoxO3a-targeted shRNA; however, we cannot rule out that possible off-target effects of this shRNA could effect the expression of other genes. To determine possible neuroprotective activity of rAAV-FoxO3a-RNAi, we exposed hippocampal neurons to NMDA, which is known to cause excitotoxic cell death via the activation of extrasynaptic NMDA receptors (1, 2, 6, 36). We found that compared with uninfected neurons or neurons infected with rAAV-control-RNAi, NMDA-induced cell death was inhibited in neurons infected with rAAV-FoxO3a-RNAi (Fig. 1B). This result indicates that expression of FoxO3a is important for excitotoxic cell death.

**Stimulation of Extrasynaptic NMDA Receptors Triggers Nuclear Translocation of FoxO3a-GFP**—Because the activity of FoxO3a as an inducer of cell death-promoting genes is dependent on its subcellular localization, we next studied the shuttling of FoxO3a between the cytosol and the nucleus. We first used antibodies to FoxO3a and immunocytochemical methods to determine the localization of endogenous FoxO3a in cultured hippocampal neurons. Cell death pathways were triggered by

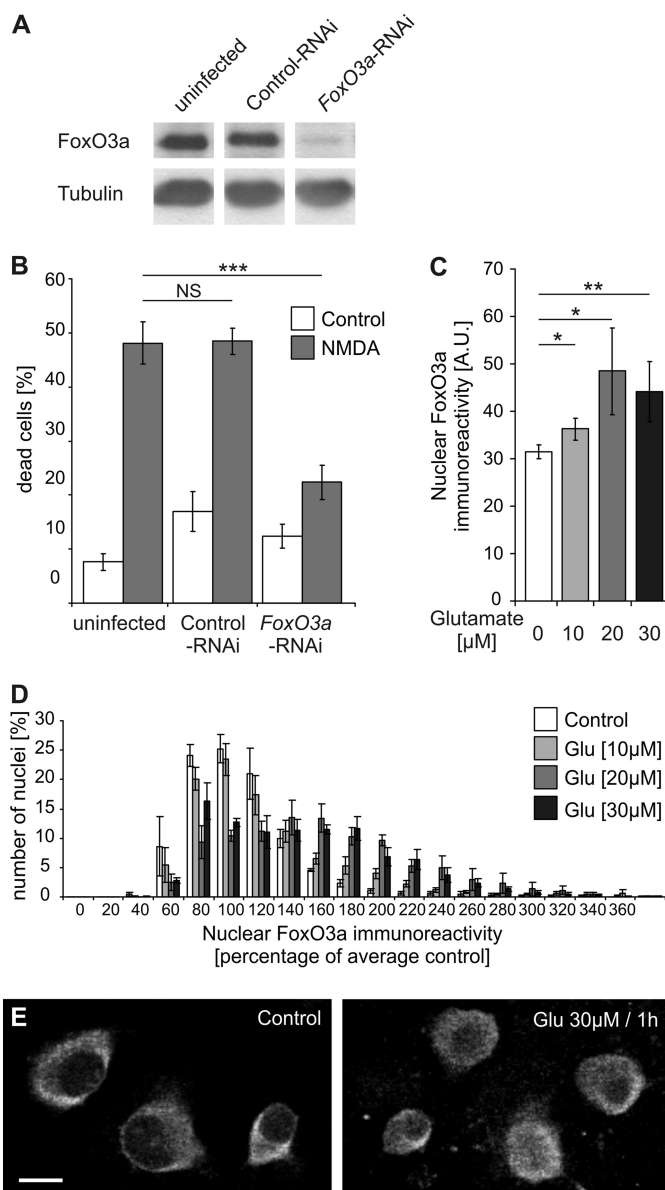


**FIGURE 1. FoxO3a is important for excitotoxicity and translocates to the nucleus upon glutamate treatment of hippocampal neurons.** A, shown is an immunoblot analysis of FoxO3a expression in uninfected hippocampal neurons and in hippocampal neurons infected with rAAV-control-RNAi or rAAV-FoxO3a-RNAi. Tubulin was used as loading control. B, shown is the analysis of cell death induced by NMDA (10  $\mu\text{M}$ ) in uninfected hippocampal neurons and in hippocampal neurons infected with rAAV-control-RNAi or rAAV-FoxO3a-RNAi. Bars represent the means  $\pm$  S.E. ( $n = 4$ ). Statistical analysis was determined by ANOVA followed by Tukey's post hoc test; \*\*\*,  $p < 0.001$ ; NS, not significant. C, quantitative analysis of nuclear FoxO3a immunoreactivity is shown. Cultured hippocampal neurons were stimulated for 1 h with the indicated concentrations of glutamate followed by immunocytochemical analysis of endogenous FoxO3a. Numbers of cells analyzed: 2651, unstimulated control; 2610, 10  $\mu\text{M}$  glutamate; 2187, 20  $\mu\text{M}$  glutamate; 3350, 30  $\mu\text{M}$  glutamate. A.U., arbitrary units. Statistically significant differences (ANOVA followed by Tukey's post hoc test) are indicated with asterisks; \*\*,  $p < 0.01$ ; \*,  $p < 0.05$ . Bars represent the means  $\pm$  S.E. ( $n = 4$ ). D, histogram showing the distribution of nuclear FoxO3a immunoreactivity in hippocampal neurons stimulated for 1 h with the indicated concentrations of glutamate as a percentage of the average intensity of untreated neurons. Numbers of cells analyzed are as in A. Bars represent the means  $\pm$  S.E. ( $n = 4$ ). E, immunostaining analysis using antibodies to FoxO3a of unstimulated hippocampal neurons (Control) and hippocampal neurons exposed for 30 min to 30  $\mu\text{M}$  glutamate. Representative examples are shown. The scale bar is 10  $\mu\text{m}$ .

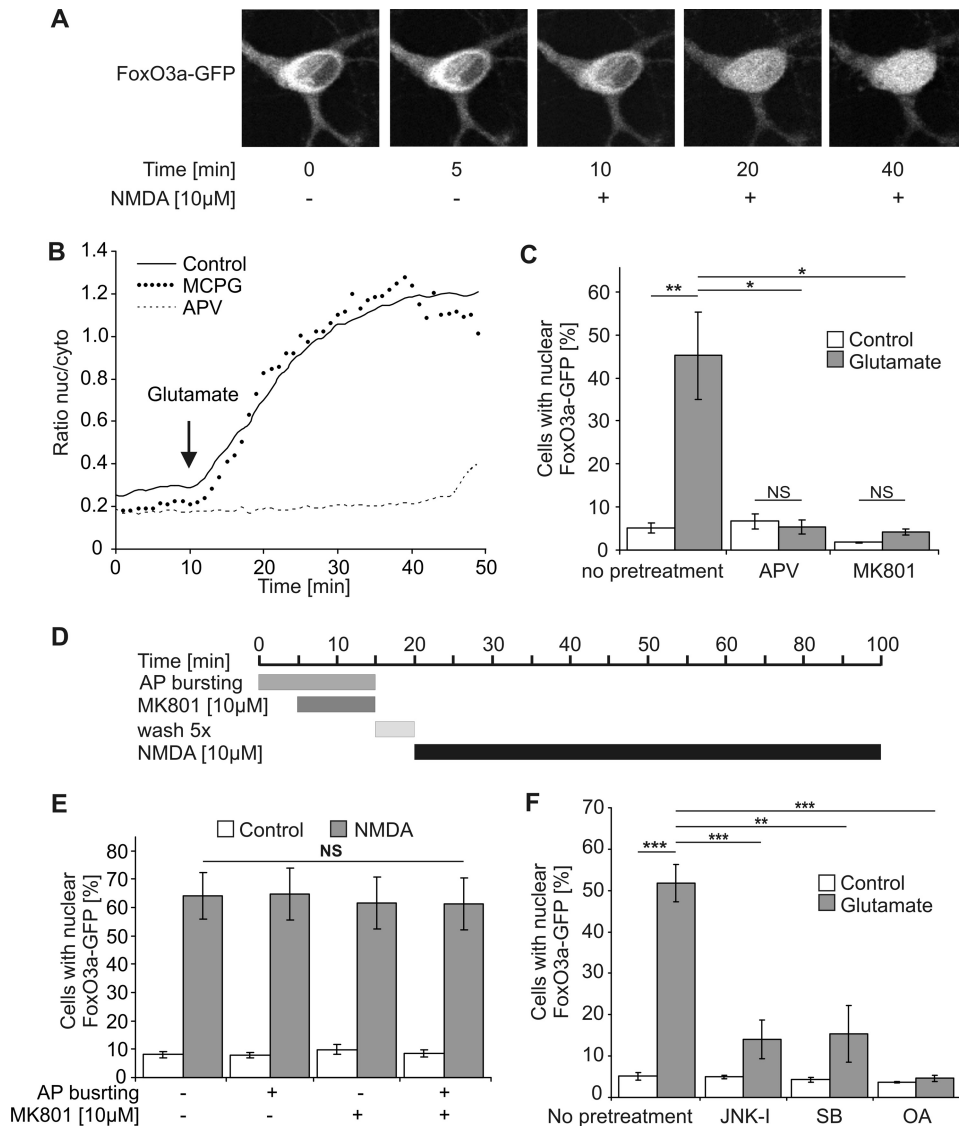


**FIGURE 2. Role of extrasynaptic NMDA receptors, JNK, p38 MAP kinase, and protein phosphatase 2A in glutamate/NMDA-induced nuclear translocation of FoxO3a-GFP.** *A*, live imaging of FoxO3a-GFP in hippocampal neurons before and after treatment with 10  $\mu$ M NMDA is shown. The confocal images are z-stacks projected into one plane and were acquired at the indicated times before and after NMDA application. A representative example is shown. *B*, shown is live imaging of FoxO3a-GFP in hippocampal neurons before and after treatment with 10  $\mu$ M glutamate in the absence of glutamate receptor blockers (solid line) or in the presence of 100  $\mu$ M APV (dashed line) or 500  $\mu$ M MCPG (dotted line). The arrow indicates the time point of glutamate application. The traces shown represent the average ratios of the nuclear and cytoplasmic FoxO3a-GFP signals obtained from four neurons (Control), five neurons (APV), and three neurons (MCPG). *nuc/cyto*, nucleo-cytoplasmic. *C*, *F*, shown is the quantitative analysis of the percentage of hippocampal neurons with nuclear localized FoxO3a-GFP. Unstimulated hippocampal neurons (Control) and hippocampal neurons stimulated for 1 h with 10  $\mu$ M glutamate were pretreated with 100  $\mu$ M APV, 10  $\mu$ M MK-801, 20  $\mu$ M JNK-1 peptide, 10  $\mu$ M SB203580 (SB), and 0.2 nM okadaic acid (OA) or received no pretreatment ( $n = 3$ ). Number of cells analyzed per condition (*i.e.* with and without glutamate stimulation): 2331, no pretreatment; 2120, APV; 2643, MK-801; 2014, JNK-1; 1963, SB203580; 2713, okadaic acid. Statistically significant differences (ANOVA followed by Tukey's post hoc test) are indicated with asterisks; \*\*\*,  $p < 0.001$ ; \*\*,  $p < 0.01$ ; \*,  $p < 0.05$ . Bars represent the means  $\pm$  S.E. ( $n = 4$ ). NS, not significant. *D*, shown is a schematic illustration of the protocol for selective stimulation of extrasynaptic NMDA receptors. *E*, shown is a quantitative analysis of the percentage of hippocampal neurons with nuclear localized FoxO3a-GFP. Neurons did or did not receive pretreatment with bicuculline/MK-801 to isolate extrasynaptic NMDA receptors and were subsequently exposed for 1 h to 10  $\mu$ M NMDA. For each condition in each experiment about 300 cells were analyzed. Statistical analysis was determined by ANOVA followed by Tukey's post hoc test; NS, not significant. Bars represent the means  $\pm$  S.E. ( $n = 5$ ).

treatment of the neurons with NMDA or glutamate. Quantitative analysis of the FoxO3a immunoreactivity of a large number of hippocampal neurons using confocal laser-scanning microscopy revealed that compared with unstimulated controls, the nuclear FoxO3a signal was significantly larger 1 h after treat-

ment of the neurons with 10, 20, and 30  $\mu$ M glutamate (Fig. 1, *C–E*). This observation indicates that FoxO3a can undergo death-signaling-associated nuclear translocation. However, the poor signal-to-noise ratio of the FoxO3a immunostaining data and the rather large cell-to-cell variability (Fig. 1, *D* and *E*) precluded an analysis of the kinetics and other properties of FoxO3a nucleo-cytoplasmic shuttling using this approach. We, therefore, transfected hippocampal neurons with an expression vector for FoxO3a fused to GFP and monitored in real time signal-regulated movements of the fusion protein. In unstimulated hippocampal neurons, FoxO3a-GFP was localized predominantly in the cytosol (Fig. 2*A*). However, upon bath application of glutamate or NMDA we observed a swift translocation of the fusion protein to the cell nucleus (Fig. 2, *A* and *B*), which in the analysis of a large population of neurons led to a robust increase in the percentage of cells with nuclear-localized FoxO3a-GFP (Fig. 2, *C*, *E*, and *F*). Using the ratio of the nuclear and cytoplasmic FoxO3a-GFP signal to quantify the shuttling, we obtained a half-maximal increase in the ratio after about 10 min; a plateau was reached after about 34 min (Fig. 2*B*). The glutamate-induced nuclear translocation of FoxO3a-GFP was blocked by the NMDA receptor antagonists, APV or MK-801, but not by MCPG, an antagonist of metabotropic glutamate receptors (mGluRs), indicating that the activation of NMDA receptors rather than mGluRs initiates the translocation (Fig. 2, *B* and *C*).

We next determined whether the cell death-promoting extrasynaptic NMDA receptors rather than synaptic NMDA receptors trigger the nuclear translocation of FoxO3a-GFP. The experimental paradigm used to isolate extrasynaptic NMDA receptors in hippocampal cultures involves MK-801 application during bicuculline-induced action potential bursting (see below) to generate a use-dependent blockade of synaptic NMDA receptors, which after wash-out of excess MK-801 allows extrasynaptic NMDA receptors to be subsequently acti-

## Nuclear Calcium and FoxO3a Shuttling

vated with bath applied NMDA (Fig. 2D) (1, 36). We found that under these conditions, NMDA treatment causes a robust nuclear translocation of FoxO3a-GFP that is indistinguishable from the translocation observed in hippocampal neurons without bicuculline/MK-801 pretreatment (Fig. 2E). This indicates that the activation of extrasynaptic NMDA receptors causes FoxO3a-GFP nuclear translocation.

Several signaling molecules and pathways have been implicated in the regulation of the subcellular distribution of FoxO3a in various cell types (37–40), among them JNK (41, 42), the p38 MAP kinase (43), and protein phosphatase 2A (44). We found that pharmacological inhibition of JNK, p38 MAP kinase, or protein phosphatase 2A using the JNK-1 inhibitor peptide, SB203580, and okadaic acid, respectively, blocked glutamate-induced nuclear translocation of FoxO3a-GFP in hippocampal neurons (Fig. 2F). These results indicate that the known regulators of FoxO3a localization also control FoxO3a shuttling in hippocampal neurons.

**Synaptic Activity Prevents Death Signal-induced Nuclear Translocation of FoxO3a-GFP**—Neuronal activity and the stimulation of synaptic NMDA receptors can boost neuroprotection and renders hippocampal neurons more resistant to harmful conditions (1, 3, 4, 6, 7, 31). We, therefore, investigated the possibility that synaptic activity before glutamate treatment could prevent the death-signal induced nuclear translocation of FoxO3a-GFP. Synaptic activity was induced by exposing the hippocampal cultures to the  $\gamma$ -aminobutyric acid (GABA), type A receptor blocker, bicuculline. This treatment relieved tonic, GABA, type A receptor-mediated inhibition of synaptic transmission from the hippocampal network, which contains about 11% GABAergic interneurons (45), and induced periodically occurring bursts of action potential (AP) firing. Each burst is associated with a robust intracellular calcium transient that propagates to the cell nucleus, stimulates CBP (cAMP-response element-binding protein (CREB)-binding protein)-mediated gene expression, and induces a genomic neuroprotective program (1, 3, 4, 6, 7, 31). We found that in hippocampal cultures treated for 16 h with bicuculline, the percentage of neurons that show nuclear translocation of FoxO3a-GFP upon exposure to 10  $\mu$ M glutamate was significantly reduced (Fig. 3A). This AP bursting-mediated protection from death signal-induced FoxO3a-GFP translocation became smaller at higher concentrations of glutamate (Fig. 3A). Glutamate concentrations lower than 10  $\mu$ M did not increase the percentage of neurons with nuclear translocation of FoxO3a-GFP above that was observed without glutamate challenge, although the 16-h period of AP bursting appeared to reduce the basal rate of neurons with nuclear-localized FoxO3a-GFP (Fig. 3A).

To investigate whether AP bursting protects from FoxO3a-GFP nuclear translocation induced by death-promoting stimuli other than glutamate exposure, we tested growth factor (GF) withdrawal and OGD, two well established death-inducing conditions (20, 46, 47). Both paradigms promoted nuclear translocation of FoxO3a-GFP, which was inhibited in cultures that had undergone a period of 16 h of AP bursting before growth factor withdrawal and OGD (Fig. 3, B and C). These results suggest that synaptic activity can lead to the

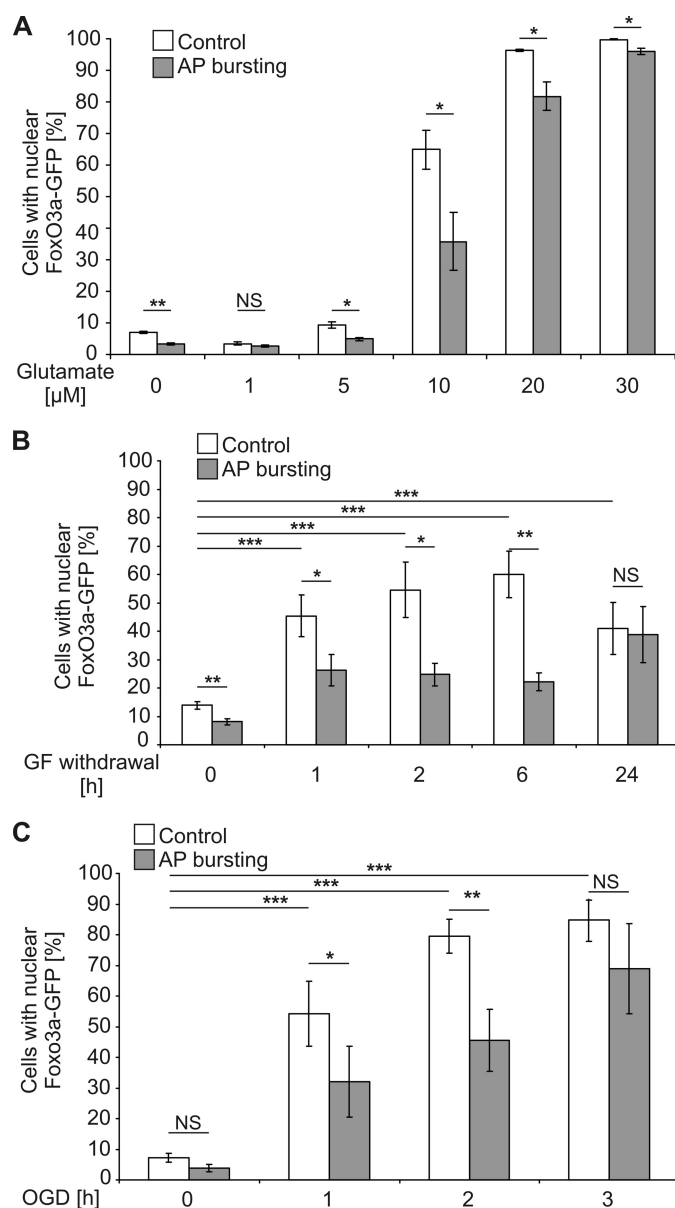


**FIGURE 3. Synaptic activity inhibits nuclear translocation of FoxO3a-GFP induced by cell death-promoting stimuli.** Shown is a quantitative analysis of the percentage of hippocampal neurons with nuclear localized FoxO3a-GFP in cultures without exposure to a cell death-promoting stimulus or in cultures after stimulation for 1 h with the indicated glutamate concentrations (A), withdrawal of growth factors (GF) for the indicated times (B), or OGD for the indicated times (C). Before application of cell death-inducing stimuli, hippocampal neurons were treated for 16 h with 50  $\mu$ M bicuculline to induce AP bursting or received no pretreatment (Control). Numbers of cells analyzed per condition (*i.e.* with and without cell death-inducing stimuli and with and without AP bursting): 9870, glutamate ( $n = 3$ ); 12638, growth factor withdrawal ( $n = 6$ ); 7941, OGD ( $n = 4$ ). Statistically significant differences (ANOVA followed by Tukey's post hoc test) are indicated with asterisks; \*\*\*,  $p < 0.001$ ; \*\*,  $p < 0.01$ ; \*,  $p < 0.05$ . NS, not significant. Bars represent the means  $\pm$  S.E. ( $n = 5$ ).

buildup of a protective shield that prevents FoxO3a-GFP from translocating to the nucleus after activation of cell death pathways.

**Activity-dependent Protection from Death Signal-induced Nuclear Translocation of FoxO3a-GFP Requires Nuclear Calcium-CaMKIV Signaling**—To gain mechanistic insight into the activity-induced modulation of FoxO3a-GFP shuttling, we first

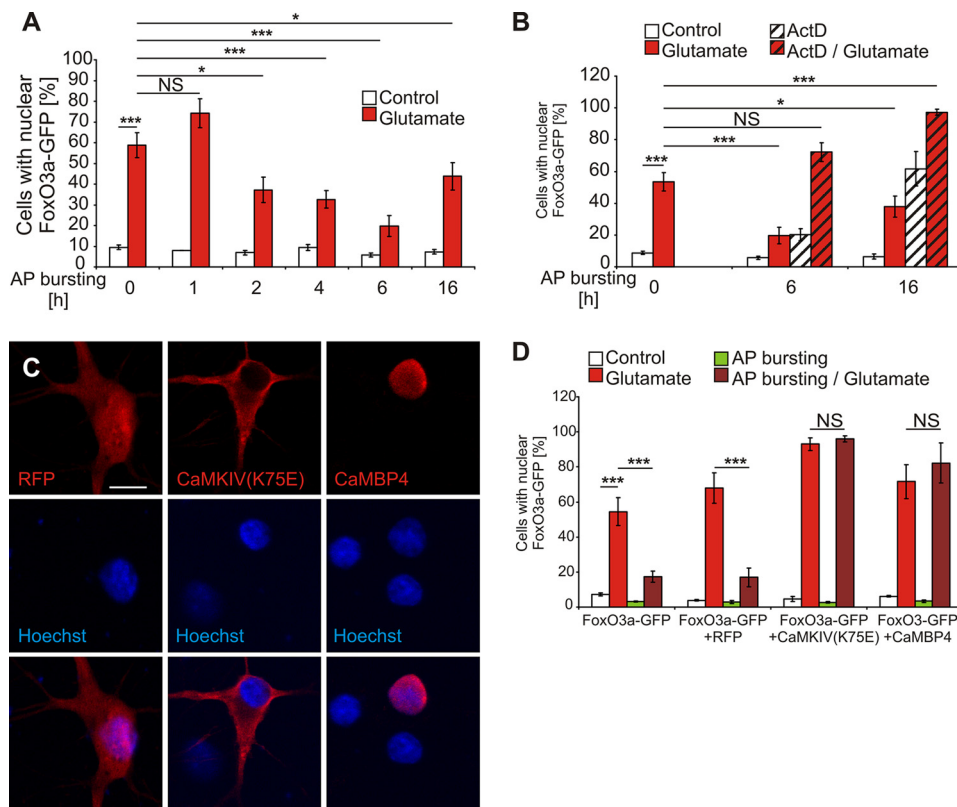


**FIGURE 4. Synaptic activity-induced protection against FoxO3a-GFP nuclear translocation after glutamate treatment requires nuclear calcium-CaMKIV signaling.** *A* and *B*, shown is a quantitative analysis of the percentage of hippocampal neurons with nuclear localized FoxO3a-GFP in unstimulated hippocampal neurons (*Control*) and hippocampal neurons stimulated for 1 h with 10  $\mu$ M glutamate in the absence or presence of actinomycin D (*ActD*; 10  $\mu$ g/ml). Before application of glutamate, hippocampal neurons were treated for the indicated times with 50  $\mu$ M bicuculline to induce AP bursting or received no pretreatment. Numbers of cells analyzed: 28930 in *A*,  $n = 5$ ; 21598 in *B*,  $n = 3$ . *NS*, not significant. *C*, shown is an immunocytochemical analysis of expression of CaMKIV(K75E), CaMBP4, and red fluorescence protein (*RFP*) in hippocampal neurons transfected with the appropriate expression vectors. Hoechst staining was used to identify nuclei. Representative confocal microscopy images are shown. CaMBP4 localizes to the cell nucleus, whereas CaMKIV(K75E) is expressed in the cytosol as has been described (61). The *Scale bar* is 10  $\mu$ m. *D*, shown is a quantitative analysis of the percentage of hippocampal neurons with nuclear localized FoxO3a-GFP in hippocampal neurons transfected with an expression vector for FoxO3a-GFP or in hippocampal neurons co-transfected an expression vector for FoxO3a-GFP and expression vectors for the indicated proteins. Hippocampal neurons were stimulated for 1 h with 10  $\mu$ M glutamate or were left unstimulated. Before application of glutamate, hippocampal neurons were treated for 16 h with 50  $\mu$ M bicuculline to induce AP bursting or received no pretreatment. Numbers of cells analyzed: 7887, no co-transfection; 7245, red fluorescence protein; 7261, CaMKIV(K75E); 5272, CaMBP4. Statistically significant differences (ANOVA followed by Tukey's post hoc test) are indicated with asterisks; \*\*\*,  $p < 0.001$ . *NS*, not significant. *Bars* represent the means  $\pm$  S.E. ( $n = 4$ ).

determined the minimum length of the AP bursting period needed to obtain a protective effect. We found that a period of 2 h of AP bursting already yielded a significant inhibitory effect; maximum protection against glutamate-induced FoxO3a-GFP nuclear translocation was obtained with a period of 6 h of AP bursting (Fig. 4A). The finding that the AP bursting-induced protective effect required several hours to be built up suggested that activity-induced gene transcription is involved. Indeed, we found that blockade of gene transcription using actinomycin D completely eliminated the ability of a 6- or 16-h lasting period of AP bursting to prevent glutamate-induced FoxO3a-GFP nuclear translocation (Fig. 4B). A possible complication in the interpretation of the results is the observation that treatment with actinomycin D alone increased slightly at the 6-h time point and dramatically at the 16-h time point the percentage of cells with nuclear-localized FoxO3a-GFP (Fig. 4B). This is not unexpected as the complete blockade of gene transcription is

harmful to the cells and as such represents a death-promoting signal that is predicted to be associated with (or even cause) FoxO3a-GFP nuclear translocation. Thus, given the combination of two death-promoting events in this experiment (*i.e.* treatment with glutamate and actinomycin D), we cannot rule out the possibility that the AP bursting-induced protection, despite the long delay until its manifestation, involves a transcription-independent process that is too weak to prevent FoxO3a-GFP nuclear translocation induced by glutamate plus actinomycin D.

To further investigate the possible importance of nuclear events in AP-bursting-induced protection, we tested the possibility that nuclear calcium signaling is critical. Calcium signals initiated by AP bursting are known to propagate toward the cell soma, where they subsequently invade the cell nucleus (30, 48). Indeed, nuclear calcium has emerged as a key mediator of synapse-to-nucleus communication; it links in a complex with the calcium sensor, CaM, neuronal activity to the regulation of gene expression important for several adaptive processes (3, 6–8, 30, 49, 50). Recently, a nuclear calcium-CaM-regulated gene pool has been identified that consists of 185 genes, among them a gene program for acquired neuroprotection (7). To interfere with nuclear calcium-CaM signaling, we expressed CaMBP4 in hippocampal

neurons. CaMBP4 is a nuclear protein that consists of four repeats of the M13 CaM-binding peptide derived from the myosin light chain kinase; it binds to and inactivates the nuclear calcium-CaM complex (34). We found that expression of CaMBP4, which is restricted to the cell nucleus (Fig. 4C) but not expression of red fluorescent protein (Fig. 4C), abolished the ability of a 16-h period of AP bursting to protect against glutamate-induced nuclear translocation of FoxO3a-GFP (Fig. 4D). These results reveal a function for nuclear calcium signaling in the protective activity afforded by AP bursting. Because many effects of nuclear calcium on transcription are mediated by the nuclear localized calcium-CaM-dependent protein kinase IV (50–56), we finally investigated the contribution of CaMKIV to AP bursting-induced protection. We found that similar to the results obtained with CaMBP4, expression of CaMKIV(K75E) (Fig. 4C), a dominant negative mutant of CaMKIV (33) blocked the build-up of protective activity during the 16-h period of AP

## Nuclear Calcium and FoxO3a Shuttling

bursting (Fig. 4D). These results establish a role of nuclear calcium-CaMKIV signaling in the modulation of FoxO3a-GFP shuttling by AP bursting.

### DISCUSSION

This study revealed that a nuclear calcium-CaMKIV mediated process initiated by AP bursting leads to the protection of hippocampal neurons from death signal-induced translocation of FoxO3a-GFP to the cell nucleus. Given the delay time for expression of the protective activity and the finding that nuclear events are critical, it is likely that nuclear calcium-CaMKIV acts via gene transcription to modulate FoxO3a-GFP shuttling. The results obtained in the actinomycin D experiment are consistent with this hypothesis, although they do not rule out possible transcription-independent processes (see above).

A comprehensive picture of genes induced or repressed by AP bursting in cultured hippocampal neurons is available (6). Moreover, a subset of 185 genes that are controlled by nuclear calcium-CaM signaling has been identified (7). Several members of the family of dual-specificity phosphatases (DUSPs) are induced by AP bursting, two of which (DUSP1 and DUSP16) in a nuclear calcium-dependent manner (6, 7). DUSPs dephosphorylate threonine and tyrosine residues on mitogen-activated protein kinases, including extracellular signal-regulated kinase-MAP kinases, p38 MAP kinases, and JNK, thereby inactivating these enzymes (37, 57). In particular, the JNK pathway has been linked to signal-regulated nuclear translocation of FoxOs (19, 27, 58). For example, in several non-neuronal cell types, nuclear translocation of FoxO4 after oxidative stress is caused by JNK-mediated phosphorylation of FoxO4 on threonine 447 and 451 (59). Although threonine 447 and 451 are not conserved among other members of the FoxO family, cellular stress conditions lead to the phosphorylation of FoxO3a within its C-terminal part on several sites that resemble potential JNK phosphorylation sites (15). An additional mechanism through which JNK affects the subcellular localization of FoxO3a involves JNK-mediated phosphorylation of 14-3-3 at serine 184, which causes dissociation of FoxO3a from 14-3-3 in the cytoplasm and nuclear translocation of FoxO3a (42). Our study has revealed the importance of JNK and p38 MAP kinase for FoxO3a-GFP shuttling in hippocampal neurons inasmuch as inhibition of either JNK or p38 MAP kinase blocked glutamate-induced nuclear translocation of FoxO3a (see Fig. 2D).

A transcriptional program that attenuates JNK or p38 MAP kinase activity could possibly explain the inhibition by AP bursting of the glutamate-induced nuclear translocation of FoxO3a. DUSP1 and DUSP16 as well as the DUSP5, -6, -10, and -14, which are also induced by AP bursting (6), could be part of this program. In addition, down-regulation of *ralgps2* after AP bursting (6) may contribute to the protective activity. *ralgps2* encodes a guanine nucleotide exchange factor for Ral, a Ras-related GTPase (60), which is required in some cell types for stress-induced JNK activation and subsequent nuclear translocation of FoxO4 (59). The available transcriptome data from cultured hippocampal neurons suggest a condition of reduced p38 MAP kinase and/or JNK activities after AP bursting; however, analysis of the phosphorylation of p38 MAP kinase and

JNK, which is indicative of their enzymatic activities, are not in line with the prediction. In immunoblot analysis, the glutamate-induced increase in p38 MAP kinase phosphorylation on threonine 180 and tyrosine 182 was not altered after a 16-h period of AP bursting (data not shown); in addition, the basal level of the phospho-JNK signal (phosphothreonine 183/phosphotyrosine 185) was high, did not increase further after glutamate exposure (as has been reported previously in (55)), and neither the basal level of phospho-JNK immunoreactivity nor the levels obtained after glutamate treatment were affected by a 16-h period of AP bursting (data not shown). However, these observations do not rule out a possible role for DUSPs and/or *ralgps2* in the protective activity against glutamate-induced nuclear translocation of FoxO3a afforded by AP bursting. DUSPs and *ralgps2* may not be homogeneously distributed within cells (37, 57) and may, therefore, only inactivate a subset of p38 MAP kinase and JNK. Such a subset (for example the cytoplasmic fraction) may contain the p38 MAP kinase and/or JNK molecules that is functionally relevant for triggering the glutamate-induced nuclear translocation of FoxO3a, yet their inactivation may not yield a detectable reduction of the overall phospho-p38 MAP kinase or phospho-JNK signals. Further studies taking into account also other genes and alternative protective mechanisms are necessary to determine precisely how AP bursting leads to the modulation of FoxO3a shuttling.

*Acknowledgments*—We thank Iris Bünzli-Ehret for preparing the hippocampal cell cultures, David Lau for help with the cloning of the rAAV constructs, M. P. Smith for a FoxO3a-GFP construct, and Thomas Dresbach for the expression vector for a red fluorescence protein.

### REFERENCES

1. Hardingham, G. E., Fukunaga, Y., and Bading, H. (2002) *Nat. Neurosci.* **5**, 405–414
2. Hardingham, G. E., and Bading, H. (2003) *Trends Neurosci.* **26**, 81–89
3. Papadia, S., Stevenson, P., Hardingham, N. R., Bading, H., and Hardingham, G. E. (2005) *J. Neurosci.* **25**, 4279–4287
4. Lee, B., Butcher, G. Q., Hoyt, K. R., Impy, S., and Obrietan, K. (2005) *J. Neurosci.* **25**, 1137–1148
5. Bok, J., Wang, Q., Huang, J., and Green, S. H. (2007) *Mol. Cell. Neurosci.* **36**, 13–26
6. Zhang, S. J., Steijaert, M. N., Lau, D., Schütz, G., Delucinge-Vivier, C., Descombes, P., and Bading, H. (2007) *Neuron* **53**, 549–562
7. Zhang, S. J., Zou, M., Lu, L., Lau, D., Ditzel, D. A., Delucinge-Vivier, C., Aso, Y., Descombes, P., and Bading, H. (2009) *PLoS Genet* **5**, e1000604
8. Limbäck-Stokin, K., Korzus, E., Nagaoka-Yasuda, R., and Mayford, M. (2004) *J. Neurosci.* **24**, 10858–10867
9. Durham, S. K., Suwanichkul, A., Scheimann, A. O., Yee, D., Jackson, J. G., Barr, F. G., and Powell, D. R. (1999) *Endocrinology* **140**, 3140–3146
10. Arden, K. C., and Biggs, W. H., 3rd. (2002) *Arch. Biochem. Biophys.* **403**, 292–298
11. Burgering, B. M., and Kops, G. J. (2002) *Trends Biochem. Sci.* **27**, 352–360
12. Burgering, B. M., and Medema, R. H. (2003) *J. Leukoc. Biol.* **73**, 689–701
13. Accili, D., and Arden, K. C. (2004) *Cell* **117**, 421–426
14. Arden, K. C. (2004) *Mol. Cell* **14**, 416–418
15. Calnan, D. R., and Brunet, A. (2008) *Oncogene* **27**, 2276–2288
16. Coffey, P. J., and Burgering, B. M. (2004) *Nat. Rev. Immunol.* **4**, 889–899
17. Furukawa-Hibi, Y., Kobayashi, Y., Chen, C., and Motoyama, N. (2005) *Antioxid. Redox Signal.* **7**, 752–760
18. Greer, E. L., and Brunet, A. (2005) *Oncogene* **24**, 7410–7425
19. Vogt, P. K., Jiang, H., and Aoki, M. (2005) *Cell Cycle* **4**, 908–913

20. Brunet, A., Bonni, A., Zigmond, M. J., Lin, M. Z., Juo, P., Hu, L. S., Anderson, M. J., Arden, K. C., Blenis, J., and Greenberg, M. E. (1999) *Cell* **96**, 857–868
21. Dijkers, P. F., Birkenkamp, K. U., Lam, E. W., Thomas, N. S., Lammers, J. W., Koenderman, L., and Coffey, P. J. (2002) *J. Cell Biol.* **156**, 531–542
22. Stahl, M., Dijkers, P. F., Kops, G. J., Lens, S. M., Coffey, P. J., Burgering, B. M., and Medema, R. H. (2002) *J. Immunol.* **168**, 5024–5031
23. Modur, V., Nagarajan, R., Evers, B. M., and Milbrandt, J. (2002) *J. Biol. Chem.* **277**, 47928–47937
24. Al-Mubarak, B., Soriano, F. X., and Hardingham, G. E. (2009) *Channels* **3**, 233–238
25. Tran, H., Brunet, A., Griffith, E. C., and Greenberg, M. E. (2003) *Sci. STKE* **2003**, RE5
26. Morris, B. J. (2005) *J. Hypertens.* **23**, 1285–1309
27. Mukhopadhyay, A., Oh, S. W., and Tissenbaum, H. A. (2006) *Exp. Gerontol.* **41**, 928–934
28. Bading, H., and Greenberg, M. E. (1991) *Science* **253**, 912–914
29. Bading, H., Segal, M. M., Sucher, N. J., Dudek, H., Lipton, S. A., and Greenberg, M. E. (1995) *Neuroscience* **64**, 653–664
30. Hardingham, G. E., Arnold, F. J., and Bading, H. (2001) *Nat. Neurosci.* **4**, 261–267
31. Lau, D., and Bading, H. (2009) *J. Neurosci.* **29**, 4420–4429
32. Potente, M., Urbich, C., Sasaki, K., Hofmann, W. K., Heeschen, C., Aicher, A., Kollipara, R., DePinho, R. A., Zeiher, A. M., and Dimmeler, S. (2005) *J. Clin. Invest.* **115**, 2382–2392
33. Anderson, K. A., Ribar, T. J., Illario, M., and Means, A. R. (1997) *Mol. Endocrinol.* **11**, 725–737
34. Wang, J., Campos, B., Jamieson, G. A., Jr., Kaetzel, M. A., and Dedman, J. R. (1995) *J. Biol. Chem.* **270**, 30245–30248
35. Bading, H., Ginty, D. D., and Greenberg, M. E. (1993) *Science* **260**, 181–186
36. Bengtson, C. P., Dick, O., and Bading, H. (2008) *BMC Neurosci.* **9**, 11
37. Patterson, K. I., Brummer, T., O'Brien, P. M., and Daly, R. J. (2009) *Biochem. J.* **418**, 475–489
38. Kau, T. R., Schroeder, F., Ramaswamy, S., Wojciechowski, C. L., Zhao, J. J., Roberts, T. M., Clardy, J., Sellers, W. R., and Silver, P. A. (2003) *Cancer Cell* **4**, 463–476
39. Hu, Y., Wang, X., Zeng, L., Cai, D. Y., Sabapathy, K., Goff, S. P., Firpo, E. J., and Li, B. (2005) *Mol. Biol. Cell* **16**, 3705–3718
40. Mattila, J., Kallijärvi, J., and Puig, O. (2008) *Proc. Natl. Acad. Sci. U.S.A.* **105**, 14873–14878
41. Barthélémy, C., Henderson, C. E., and Pettmann, B. (2004) *BMC Neurosci.* **5**, 48
42. Sunayama, J., Tsuruta, F., Masuyama, N., and Gotoh, Y. (2005) *J. Cell Biol.* **170**, 295–304
43. Dávila, D., and Torres-Aleman, I. (2008) *Mol. Biol. Cell* **19**, 2014–2025
44. Bertoli, C., Copetti, T., Lam, E. W., Demarchi, F., and Schneider, C. (2009) *Oncogene* **28**, 721–733
45. Arnold, F. J., Hofmann, F., Bengtson, C. P., Wittmann, M., Vanhoutte, P., and Bading, H. (2005) *J. Physiol.* **564**, 3–19
46. Won, C. K., Ji, H. H., and Koh, P. O. (2006) *Neurosci. Lett* **398**, 39–43
47. Chong, Z. Z., and Maiese, K. (2007) *Br. J. Pharmacol.* **150**, 839–850
48. Eder, A., and Bading, H. (2007) *BMC Neurosci.* **8**, 57
49. Hardingham, G. E., Chawla, S., Johnson, C. M., and Bading, H. (1997) *Nature* **385**, 260–265
50. Chawla, S., Hardingham, G. E., Quinn, D. R., and Bading, H. (1998) *Science* **281**, 1505–1509
51. Enslin, H., Sun, P., Brickey, D., Soderling, S. H., Klamo, E., and Soderling, T. R. (1994) *J. Biol. Chem.* **269**, 15520–15527
52. Matthews, R. P., Guthrie, C. R., Wailes, L. M., Zhao, X., Means, A. R., and McKnight, G. S. (1994) *Mol. Cell Biol.* **14**, 6107–6116
53. Means, A. R., Ribar, T. J., Kane, C. D., Hook, S. S., and Anderson, K. A. (1997) *Recent Prog. Horm. Res.* **52**, 389–407
54. Agell, N., Bachs, O., Rocamora, N., and Villalonga, P. (2002) *Cell Signal* **14**, 649–654
55. Hardingham, G. E., Chawla, S., Cruzalegui, F. H., and Bading, H. (1999) *Neuron* **22**, 789–798
56. Hook, S. S., and Means, A. R. (2001) *Annu. Rev. Pharmacol. Toxicol.* **41**, 471–505
57. Jeffrey, K. L., Camps, M., Rommel, C., and Mackay, C. R. (2007) *Nat. Rev. Drug Discov.* **6**, 391–403
58. Huang, H., and Tindall, D. J. (2007) *J. Cell Sci.* **120**, 2479–2487
59. Essers, M. A., Weijzen, S., de Vries-Smits, A. M., Saarloos, I., de Ruiter, N. D., Bos, J. L., and Burgering, B. M. (2004) *EMBO J.* **23**, 4802–4812
60. Rebhun, J. F., Chen, H., and Quilliam, L. A. (2000) *J. Biol. Chem.* **275**, 13406–13410
61. Chow, F. A., Anderson, K. A., Noeldner, P. K., and Means, A. R. (2005) *J. Biol. Chem.* **280**, 20530–20538